Spectroscopic and Photophysical Properties of Complexes of 4′-Ferrocenyl-2,2′:6′,2″-terpyridine and Related Ligands

Kimberly Hutchison, James C. Morris, Terence A. Nile, and Jerry L. Walsh*

Department of Chemistry, University of North Carolina at Greensboro, Greensboro, North Carolina 27412

David W. Thompson[†] **and John D. Petersen***

Department of Chemistry, Wayne State University, Detroit, Michigan 48202

Jon R. Schoonover*

Los Alamos National Laboratories, Los Alamos, New Mexico 87545

Received July 10, 1998

4′-(Ferrocenyl)-2,2′:6′,2″-terpyridine (Fctpy) and 4′-(4-pyridyl)-2,2′:6′,2″-terpyridine (pytpy) were prepared from the corresponding ferrocene- and pyridinecarboxaldehyle and 2-acetylpyridine using the Krohnke synthetic methodology. Metal complexes, $[M(Fctpy)_2](PF_6)_2$ (M = Ru, Fe, Zn), $[Ru(tpy)(Fctpy)](PF_6)_2$ (tpy = 2,2′:6′,6″-terpyridine), and $[Ru(pytpy)_2](PF_6)_2$ were prepared and characterized. Cyclic voltammetric analysis indicated $Ru^{III/II}$ and ferrocenium/ferrocene redox couples near expected potentials ($Ru^{III/II}$ ∼1.3 V and ferrocenium/ferrocene ∼0.6 V vs Ag/AgCl). In addition to dominant $\pi_{tpy} \rightarrow \pi_{tpy}^*$ UV absorptions near 240 and 280 nm and $d_\pi^{Ru} \rightarrow \pi_{tpy}^*$ MLCT absorptions around 480 nm, the complexes $[Ru(Fctpy)_2](PF_6)_2$ and $[Ru(tpy)(Fctpy)](PF_6)_2$ exhibit an unusual absorption band around 530 nm. Resonance Raman measurements indicate that this band is due to a $^1[(d(\pi)_{Fc})^6] \rightarrow {}^1[(d(\pi)_{Fc})^5(\pi^*_{tpy}{}^{Ru})^1]$ transition. For $[Ru(Fctpy)_2](PF_6)_2$ and $[Ru(tpy)(Fctpy)](PF_6)_2$, excited-state emission and lifetime measurements indicated an upper-limit emission quantum yield of 0.003 and an upper-limit emission lifetime of 0.025 μs. The influence of the ferrocenyl site on excited-state decay is discussed, and an excited-state energy level diagram is proposed.

Introduction

Polypyridyl ruthenium(II) complexes have been the basis for numerous studies of ground- and excited-state spectra, electron transfer, and photochemical reactions.[1−5] A wide variety of ligands have been utilized in these studies, illustrating that redox potentials, absorption spectra, electron delocalization, excited-state energies, and relaxation processes can be systematically controlled. Interest in the synthesis of unique ligands and the properties of ruthenium(II) complexes containing these ligands remains high.[5−26] In particular, ruthenium complexes of substituted terpyridines (tpy) show considerable variation in photophysical properties.[6−15,19−23] Species containing redox-active moieties attached to terpyridine are of particular interest[11−17,22−24]

[†] Present address: Department of Chemistry, Johns Hopkins University, 3400 N. Charles St., Baltimore, MD 21218.

(1) Kalyanasundaram, K. *Photochemistry of Polypyridine and Porphyryn Complexes*; Academic: London, 1992.
(2) Meyer, T. J. *Pure Appl. Chem.* **1986**, *58*, 1193.
(3) Kalyanasundaram, K. *Coord. Chem. Rev.* **1982**, *46*, 159.
(4) Meyer, T. J. *Acc. Chem. Res.* **1989**, *22*, 163.
(5) Balzani, V.; Scandola, F. *Supramolecular Photochemistry*; Ellis Harwood: Chichester, U.K., 1991.
(6) Constable, E. C. *Prog. Inorg. Chem.* **1994**, *42*, 67.
(7) Constable, E. C.; Cargill Thompson, A. M. W.; Tocher, D. A. *Supramol. Chem.* **1993**, *3*, 9.
(8) Constable, E. C.; Hannon, M. J.; Cargill Thompson, A. M. W.; Tocher, D. A.; Walker, J. V. *Supramol. Chem.* **1993**, *2*, 243.
(9) Beley, M.; Chodoroski, S.; Collin, J.-P.; Sauvage, J.-P.; Flamigni, L.; Barigelletti, F. *Inorg. Chem.* **1994**, *33*, 2543 and references therein.
(10) Sauvage, J.-P.; Collin, J.-P.; Chambron, J.-C.; Guillerez, S.; Coudret, C.; Balzani, V.; Barigelletti, F.; De Cola, L.; Flamigni, L. *Chem. Rev.* **1994**, *94*, 993.
(11) Farlow, B.; Nile, T. A.; Walsh, J. L.; McPhail, A. T. *Polyhredon* **1993**, *12*, 2891.
(12) Constable, E. C.; Edwards, A. J.; Martinez-Máñez, R.; Raithby, P. R.; Cargill Thompson, A. M. W. *J. Chem. Soc., Dalton Trans.* **1994**, 645.
(13) Constable, E. C.; Edwards, A. J.; Martinez-Máñez, R.; Raithby, P. R. *J. Chem. Soc., Dalton Trans.* **1995**, 3253.
(14) Constable, E. C.; Edwards, A. J.; Martinez-Máñez, R.; Cargill Thompson, A. M. W.; Walker, J. V. *J. Chem. Soc., Dalton Trans.* **1994**, 1585.
(15) Constable, E. C.; Cargill Thompson, A. M. W. *J. Chem. Soc., Dalton Trans.* **1992**, 3467.
(16) Constable, E. C.; Cargill Thompson, A. M. W.; Tocher, D. A.; Daniels, M. A. M. *New J. Chem.* **1992**, *16*, 855.
(17) Collin, J.-P.; Guillerez, S.; Sauvage, J.-P.; Barigelletti, F.; De Cola, L.; Flamigni, L.; Balzani; V. *Inorg. Chem.* **1991**, *30*, 4230.
(18) Maestri, M.; Armaroli, N.; Balzani, V.; Constable, E. C.; Cargill Thompson, A. M. W. *Inorg. Chem.* **1995**, *34*, 2759.
(19) Constable, E. C.; Cargill Thompson, A. M. W.; Armaroli, N.; Balzani, V.; Maestri, M. *Polyhedron* **1992**, *11*, 2707.
(20) Constable, E. C.; Cargill Thompson, A. M. W. *J. Chem. Soc., Dalton Trans.* **1992**, 2947.
(21) Constable, E. C.; Cargill Thompson, A. M. W. *J. Chem. Soc., Dalton Trans.* **1994**, 1409.
(22) Constable, E. C.; Edwards, A. J.; Marcos, M. D.; Raithby, P. R.; Martinez-Máñez, R.; Tendero, M. J. L. *Inorg. Chim. Acta* **1994**, *224*, 11.
(23) Butler, I. R.; McDonald, S. J.; Hursthouse, M. B.; Abdul Malik, K. M. *Polyhedron* **1995**, *14*, 529.
(24) Chambron, J.-C.; Coudret, C.; Sauvage, J.-P. *New J. Chem.* **1992**, *16*, 361.

10.1021/ic980798b CCC: $18.00
Published on Web 04/28/1999

because of their potential role in mediating excited-state relaxation, in molecular sensing, and in redox-active self-assembly devices. In fact, a number of polypyridyl ligands containing attached ferrocenyl moieties have been prepared.

The use of 4′-ferrocenyl- and 4′-pyridyl-2,2′:6′,2″-terpyridine ligands[11,12,20,23] (Fctpy and pytpy, respectively) in a series of coordination complexes is described here. The influence of the 4′ substituents on the ground- and excited-state properties of the ruthenium complexes are described. The characterization of an unusual absorption band in the visible spectra of certain tpy complexes and the use of resonance Raman spectra in characterizing the band are also described.

Experimental Section

Materials. Preparation of $Ru(DMSO)_4Cl_2$,[30] $[Ru(tpy)_2](PF_6)_2$,[31] $Ru(tpy)Cl_3$,[32] 4′-ferrocenyl-2,2′:6′,2″-terpyridine[11,12] (Fctpy), and 4′-(4″-pyridyl)-2,6′:2′,6″-terpyridine[20] (pytpy) followed the literature procedures. Other chemicals were reagent grade and used as received.

Preparations. $[Ru(Fctpy)_2](PF_6)_2$. Fctpy (52 mg; 0.12 mmol) was added to a solution of 30 mg (0.062 mmol) of $Ru(DMSO)_4Cl_2$ in 10 mL of ethanol. The solution was heated at reflux for 30 min. Excess NH_4PF_6(aq) was added, and the solution was cooled. The precipitate was collected, washed with ethanol and diethyl ether, and air-dried. The product was then recrystallized from an acetone/ethanol solution. Yield: 40 mg (53%). Anal. Calcd for $C_{50}H_{38}F_{12}Fe_2N_6P_2Ru$: C, 49.00; H, 3.12; N, 6.86. Found: C, 48.88; H, 3.12; N, 6.62. ^{1}H NMR (δ(ppm), acetone-d_6): 9.23 (s, 4H), 9.00 (d, 4H), 8.11 (t, 4H), 7.81 (d, 4H), 7.38 (t, 4H), 5.56 (t, 4H), 4.84 (t, 4H), 4.38 (s, 10H).

$[Ru(tpy)(Fctpy)](PF_6)_2$. $RuCl_3 \cdot xH_2O$ (180 mg; ~0.69 mmol) and tpy (161 mg; 0.69 mmol) were added to a flask containing 150 mL of ethanol. The mixture was refluxed for 3 h and then filtered. The 231 mg of precipitate thus obtained, presumably $Ru(tpy)Cl_3$, and Fctpy (113 mg; 0.27 mmol) were added to 30 mL of a 2:1 mixture of ethanol and water which contained 10 drops of triethylamine. The mixture was refluxed for 4 h and then filtered. The filtrate volume was reduced to 10 mL on a rotary evaporator, and NH_4PF_6(aq) was added until precipitation was complete. The precipitate was collected by filtration and washed with water, ethanol, and diethyl ether. The product was purified by chromatography with an alumina-packed column, with the desired product being eluted with a solvent containing 5% methanol in acetone. The volume of solvent was reduced to a few milliliters and the product was precipitated by addition of diethyl ether. Yield: 205 mg (29%). Anal. Calcd for $C_{40}H_{30}F_{12}FeN_6P_2Ru$: C, 46.13; H, 2.90; N, 8.07. Found: C, 46.19; H, 2.89; N, 7.96. ^{1}H NMR (δ(ppm), acetone-d_6): 9.24 (s, 2H), 9.11 (d, 2H), 9.01 (d, 2H), 8.85 (d, 2H), 8.60 (t, 1H), 8.11 (t, 4H), 7.84 (d, 2H), 7.71 (d, 2H), 7.38 (m, 4H), 5.56 (s, 2H), 4.84 (s, 2H), 4.39 (s, 5H).

$[Ru(pytpy)_2](PF_6)_2$. Under a nitrogen atmosphere, $AgPF_6$ (104 mg; 0.41 mmol) in 5 mL of DMSO was added to a solution of $Ru(DMSO)_4Cl_2$ (100 mg; 0.21 mmol) in 20 mL of DMSO and the mixture was heated at about 40 °C for 30 min. The mixture was filtered. The filtrate was added to a solution of 200 mg (0.65 mmol) of pytpy, and the solution was refluxed for 20 h under a nitrogen atmosphere. After cooling, the volume of solution was reduced to about 5 mL by rotary evaporation, 10 mL of water was added, and NH_4PF_6(aq) was added. The resulting precipitate was collected and air-dried. The product was dissolved in acetone and purified by chromatography with an alumina-packed column, using 10% methanol in acetone to remove the product. The solvent from the eluted fraction was removed by rotary evaporation. The product was dissolved in acetone and then precipitated by addition of the solution to diethyl ether. Yield: 47 mg (22%). Anal. Calcd for $C_{40}H_{28}F_{12}N_8P_2Ru$: C, 47.49; H, 2.79; N, 11.08. Found: C, 46.90; H, 3.02; N, 11.10. ^{1}H NMR (δ(ppm), acetone-d_6): 9.63 (s, 4H), 9.14 (d, 4H), 9.00 (d, 4H), 8.34 (d, 4H), 8.18 (t, 4H), 7.89 (d, 4H), 7.41 (t, 4H).

$[Fe(Fctpy)_2](PF_6)_2$. Ferrous ammonium sulfate hexahydrate (38 mg; 0.097 mmol) was dissolved in 5 mL of water and added slowly to 50 mL of 50/50 acetone/ethanol containing 80 mg (0.19 mmol) of Fctpy. After reducing the volume by rotary evaporation, NH_4PF_6(aq) was added until precipitation was complete. The precipitate was collected and washed with water, ethanol, and diethyl ether. The product was purified by chromatography as described above. Yield: 72 mg (63%). Anal. Calcd for $C_{50}H_{38}F_{12}Fe_3N_6P_2$: C, 50.88; H, 3.24; N, 7.12. Found: C, 50.52; H, 3.19; N, 6.97. ^{1}H NMR (δ(ppm), acetone-d_6): 9.41 (s, 4H), 8.97 (d, 4H), 8.08 (t, 4H), 7.57 (d, 4H), 7.30 (t, 4H), 5.65 (t, 4H), 4.90 (t, 4H), 4.43 (s, 5H).

$[Zn(Fctpy)_2](PF_6)_2$. Zinc acetate (50.0 mg; 0.230 mmol) was dissolved in 10 mL of water and then added to 20 mL of 50/50 acetone/ethanol which contained 208 mg (0.500 mmol) of Fctpy. After being stirred for 30 min, the solution was filtered, and NH_4PF_6(aq) was added until precipitation was complete. The precipitate was collected and washed with water and ethanol. The product was recrystallized by dissolving in acetone and adding the solution dropwise to diethyl ether. The precipitate was collected by filtration and washed with diethyl ether. Yield: 204 mg (0.167 mmol; 73%). Anal. Calcd for $C_{50}H_{38}F_{12}Fe_2N_6P_2Zn \cdot 2H_2O$: C, 48.99; H, 3.45; N, 6.86. Found: C, 48.96; H, 3.33; N, 6.85. ^{1}H NMR (δ(ppm), acetone-d_6): 9.15 (s, 4H), 9.06 (d, 4H), 8.34 (t, 4H), 8.18 (d, 4H), 7.59 (t, 4H), 5.61 (t, 4H), 4.90 (t, 4H), 4.36 (s, 10H).

General Methods. Elemental analyses were performed by Desert Analytics, Tucson, AZ. Proton NMR spectra were obtained on a Bruker Avance DRX300 spectrometer. UV−visible spectra were measured with a Varian DMS-100, Hitachi 100-80 spectrophotometer, or a Hewlett-Packard model 8451A diode array spectrophotometer interfaced to an IBM microcomputer. A Cypress Systems model CS-1087 electrochemical analyzer was used for cyclic voltammetric measurements. Electrochemical data was collected using a cell with a platinum bead working electrode, an Ag/AgCl reference electrode, and a platinum wire counter electrode. The solvent was 0.1 M tetraethylammonium perchlorate (TEAP) in acetonitrile. Bulk electrolyses were performed with a Bioanalytical Systems CV-1B potentiostat.

Photophysical Measurements. Samples for lifetime and emission experiments were prepared as optically dilute solutions (Δabs < 0.2 at the λ_{max} in a 1.00 cm cell) in freshly distilled EtOH/MeOH (4:1 (v/v)), freeze−pump−thaw degassed for at least three cycles until the pressure was below 10^{-6} Torr, and sealed under vacuum. Visible spectra were recorded on all samples before and after excited-state measurements to ensure that the samples did not photodegrade.

Emission spectra were measured with a Spex Fluorolog F212 photon-counting spectrofluorimeter equipped with a red-sensitive Hamamatsu R666-98 photomultiplier tube. All spectra were collected using a 2 mm slit width and were corrected for instrument response using a procedure supplied by the manufacturer. Emission quantum yields, Φ_{em}, were measured in optically dilute EtOH/MeOH (4:1 (v/v)) rigid glasses at 77 K relative to $Ru(tpy)_2(PF_6)_2$ for which $\Phi_{em} = 0.48$.[33−35] Quantum yields were calculated using eq 1 as described previously[36,37]

(25) Scandola, F.; Indelli, M. T.; Chiorboli, C.; Bignozzi, C. A. *Top. Curr. Chem.* **1990**, *158*, 73.
(26) Bhadbhade, M. M.; Das, A.; Jeffery, J. C.; McCleverty, J. A.; Navas Badiola, J. A.; Ward, M. D. *J. Chem. Soc., Dalton Trans.* **1995**, 2769.
(27) Butler, I. R.; Roustan, J.-L. *Can. J. Chem.* **1990**, *68*, 2212.
(28) Butler, I. R. *Organometallics* **1992**, *11*, 74.
(29) Beer, P. D.; Kocian, O.; Mortimer, R. J. *J. Chem. Soc., Dalton Trans.* **1990**, 3283.
(30) Evans, I. P.; Spencer, A.; Wilkinson, G. *J. Chem. Soc., Dalton Trans.* **1973**, 204.
(31) Braddock, J. N.; Meyer, T. J. *J. Am. Chem. Soc.* **1973**, *95*, 3158.
(32) Sullivan, B. P.; Calvert, J. M.; Meyer, T. J. *Inorg. Chem.* **1980**, *19*, 1404.
(33) Stone, M. L.; Crosby, G. A. *Chem. Phys. Lett.* **1981**, *79*, 169.
(34) Beley, M.; Collin, J.-P.; Sauvage, J.-P.; Sugihara, H.; Heisel, F.; Miehe, A. *J. Chem. Soc., Dalton Trans.* **1991**, 3157.
(35) Winkler, J. R.; Netzel, T. L.; Creutz, C.; Sutin, N. *J. Am. Chem. Soc.* **1987**, *109*, 2381.
(36) Worl, L. A.; Duesing, R.; Chen, P.; Della Ciana, L.; Meyer, T. J. *J. Chem. Soc., Dalton Trans*. **1991**, 849.
(37) Damrauer, N. H.; Boussie, T. R.; Devenney, M.; McCusker, J. K. *J. Am. Chem. Soc*. **1997**, *119*, 8253.

$$\Phi_{em} = (A_r/I_r)(I_s/A_s)(n_s/n_r)^2\Phi_r \quad (1)$$

where A is the absorbance at the excitation wavelength, I is the integrated area of the emission band, and n is the refractive index of the solvent for the sample (subscript s) and the reference (subscript r), respectively. Excitation and emission spectra were found to be independent of monitoring and excitation wavelength.

Emission lifetimes were measured at 77 K using a liquid nitrogen Dewar with a PRA LN1000 pulsed nitrogen laser as an excitation source at 337 nm, coupled to a PRA grating LN102/1000 tunable dye laser. All lifetimes were measured following 460 nm excitation using Exiton Coumarin 460 laser dye. The excitation beam was passed through a collection of lenses and defocused onto the sample cell. The incident excitation beam was directed 90° to the cell surface and emission was monitored 90° to the excitation beam with a PRA B204-3 2.5 monochromator and a Hamamatsu R 928 photomultiplier tube. Scattered light was removed by a dichromate filter solution. A LeCroy 9400 digital oscilloscope or a LeCroy 7200A digitizer was interfaced with a IBM PC microcomputer to collect the kinetic data. Rate constants for emission decay were calculated using a Marquardt nonlinear least-squares fitting procedure described previously.[38]

Time-resolved fluorescence measurements at 77 K were also attempted using a Spex Tau-2 multifrequency phase shift fluorometer. The excitation source was a 450 W xenon arc lamp. Measurements were made using a Finger Dewar provided by Spex Industries. Care was taken to ensure that Δabs < 0.2 at the λ_{exc} in a 1.00 cm cell for the luminophores in room-temperature solution. Measurements were attempted in the 100−300 MHz frequency window by sequentially collecting the emitted light from the luminophores at each specified frequency. Light scatter from the nitrogen Dewar was used as a reference.

Wavelength-dependent resonance Raman (RR) spectra for $[Ru(Fctpy)_2](PF_6)_2$ ([Ru] $\approx 10^{-4}$ M) at 298 K in CH_3CN were measured using the 457.9, 488.0, 514.5, and 568.2 nm laser lines from a Spectra-Physics model 165 Ar^+ CW laser. The scattered radiation was dispersed by a Jobin Yvon U1000 double monochromator and detected by a Hamamatsu R943-02 water-cooled photomultiplier tube. Signal processing was accomplished with an Instruments SA Spectra Link photon-counting system. The spectra were an average of 16 accumulations with a spectral resolution of 4 cm^{-1} and were uncorrected for instrument response. Reported intensities were calculated relative to the solvent Raman band at 918 cm^{-1}.

Results

Synthesis of Compounds. The bis(terpyridyl) complexes $Ru(Fctpy)_2^{2+}$ and $Ru(pytpy)_2^{2+}$ were prepared by reaction of the appropriate terpyridyl ligand with $Ru(DMSO)_4Cl_2$ in ethanol and in DMSO, respectively. A two-step process involving first generation of $Ru(tpy)Cl_3$ and then subsequent reaction with Fctpy was used to prepare $Ru(tpy)(Fctpy)^{2+}$. The other complexes, $Fe(Fctpy)_2^{2+}$ and $Zn(Fctpy)_2^{2+}$ were readily prepared by direct reaction of the metal ion with Fctpy in aqueous ethanol solution. In each case, there is a tendency for the ferrocene moiety to undergo decomposition with coordination of the released Fe^{2+} to free terpyridine moieties, as indicated by generation of a blue-purple color in solution.

Electrochemistry. Electrochemical results are listed in Table 1. The ferrocenyl moieties of Fctpy, $Ru(Fctpy)_2^{2+}$, $Ru(tpy)(Fctpy)^{2+}$, and $Fe(Fctpy)_2^{2+}$ exhibit reversible oxidation of one electron per ferrocenyl unit (eqs 2 and 3) at around 0.6 V vs Ag/AgCl. Results indicate that the ferrocenyl moiety is more

$$Ru^{II}(tpy)(Fc^{II}tpy)^{2+} \rightarrow Ru^{II}(tpy)(Fc^{III}tpy)^{3+} + e^- \quad (2)$$

difficult to oxidize by about 0.17 V than ferrocene, an effect

$$Ru^{II}(Fc^{II}tpy)_2^{2+} \rightarrow Ru^{II}(Fc^{III}tpy)_2^{4+} + 2e^- \quad (3)$$

observed for other ferrocenes with aromatic substituents.[26,39,40] The reversible reduction of the coordinated tpy moiety at around −1.2 V is relatively unperturbed by the attached ferrocenyl or pyridyl group. The $Ru^{III/II}$ couple for $Ru(Fctpy)_2^{2+}$ occurs near 1.3 V, as in $Ru(tpy)_2^{2+}$, but the wave is irreversible as evidenced by asymmetric peak heights and electrode deposition during bulk electrolysis. At this potential, oxidation to a +5 complex (a ruthenium(III) center and two ferrocenium units) occurs, resulting in product precipitation on the electrode. This behavior was not furthur investigated. Similar electrochemistry was observed in the $Fe(Fctpy)_2^{2+}$ system.

UV−Visible and Resonance Raman Spectroscopy. The UV−visible spectral data are summarized in Table 1, and the spectra of $Ru(tpy)_2^{2+}$, $Ru(tpy)(Fctpy)^{2+}$, and $Ru(Fctpy)_2^{2+}$ are compared in Figure 1. The visible absorption bands observed in the spectrum of Fc at 325 nm ($\epsilon_{325} = 51$ M^{-1} cm^{-1}) and 440 nm ($\epsilon_{440} = 87$ M^{-1} cm^{-1}) have been previously assigned to the $^1A_{1g} \rightarrow {}^1E_{1g}$ and $^1A_{1g} \rightarrow {}^1E_{2g}$ ligand-field (dd) transitions, respectively, in D_{5d} symmetry.[26,41,42] The visible bands for Fctpy at 364 ($\epsilon_{364} = 2200$ M^{-1} cm^{-1}) and 459 nm ($\epsilon_{459} = 910$ M^{-1} cm^{-1}) are red-shifted relative to Fc, and the molar absorptivities of the Fctpy bands are considerably enhanced relative to Fc, consistent with the electron-withdrawing character of tpy.[41,42]

The visible absorption spectra for $Ru(tpy)(Fctpy)^{2+}$ and $Ru(Fctpy)_2^{2+}$ shown in Figure 1 are dominated by $^1[(d(\pi)^6)] \rightarrow {}^1[(d(\pi)^5(\pi^*_{tpy})^1]$ MLCT absorption bands at 480 nm which were assigned by analogy to the well-documented MLCT transitions found for $Ru(tpy)_2^{2+}$ and $Ru(bpy)_3^{2+}$. The absorption bands are broad because they include a series of MLCT transitions and their vibronic components.[31,43,44] All the compounds investigated possess intense intraligand tpy-centered $\pi \rightarrow \pi^*$ absorption bands in the UV.

Additional broad structureless absorption bands at 515 and 526 nm for $Ru(tpy)(Fctpy)^{2+}$ and $Ru(Fctpy)_2^{2+}$, respectively, are apparent in the visible absorption spectra, spectra A and B of Figure 1. The intense band in the 530 nm region is absent in other 4′-substituted tpy complexes[9,10,18,45−47] but has been observed in other Ru(II) and Os(II) heterobimetallic complexes containing pendant Fc moieties.[10,48] For the $Ru(tpy)(Fctpy)^{2+}$ and $Ru(Fctpy)_2^{2+}$ compounds under investigation, the 515 and 526 nm transitions also involve the Fc center because the intensity of this transition scales with the number of pendant Fc substituents and the band disappears upon the oxidation of Fc (eqs 2 and 3). The appearance of a similar absorption band in $Zn(Fctpy)_2^{2+}$, $Ni(Fctpy)_2^{2+}$, and protonated Fctpy confirms that the band is related to Fctpy and not to the ruthenium center. This band appears to arise from a $^1[(d(\pi)_{Fc})^6] \rightarrow {}^1[(d(\pi)_{Fc})^5(\pi^*_{tpy}{}^{Ru})^1]$ transition analogous to other related terpyridyl assemblies.[10] This band is not present in the parent Fctpy, but

(38) Chen, P.; Duesing, R.; Graff, D. K.; Meyer, T. J. *J. Phys. Chem.* **1991**, *95*, 5850.
(39) Carugo, O.; De Santis, G.; Fabbrizzi, L.; Licchelli, M.; Monichino, A.; Pallavicini, P. *Inorg. Chem.* **1992**, *31*, 765.
(40) Sabbatini, M. M.; Cesarotti, E. *Inorg. Chim. Acta* **1977**, *24*, L9.
(41) Bozak, R. E. *Adv. Photochem.* **1971**, *8*, 227.
(42) Sohn, Y. S.; Hendrickson, D. N.; Gray, H. B. *J. Am. Chem. Soc.* **1971**, *93*, 3603.
(43) Coe, B. J.; Thompson, D. W.; Culbertson, C. T.; Schoonover, J. R.; Meyer, T. J. *Inorg. Chem.* **1995**, *34*, 3385.
(44) Kober, E. M.; Meyer, T. J. *Inorg. Chem.* **1982**, *21*, 3967.
(45) Thummel, R. P.; Hedge, V.; Jahng, Y. *Inorg. Chem.* **1989**, *28*, 3264.
(46) Hecker, C. R.; Gushurst, A. K. I.; McMillin, D. R. *Inorg. Chem.* **1991**, *30*, 538.
(47) Ben Hadda, T.; Le Bozec, H. *Polyhedron* **1988**, *7*, 575.
(48) Benniston, A. C.; Goulle, V.; Harriman, A.; Lehn, J.-M.; Marczinke, B. *J. Phys. Chem.* **1994**, *98*, 7798.

Table 1. UV−Visible and $E_{1/2}$ Data at 293(3) K

compound	$E_{1/2}$, V vs Ag/AgCl				absorption data, λ_{max}, nm (ϵ, $\times 10^{-3}$ M^{-1} cm^{-1})
	$Ru^{III/II}$	$Fc^{+/0}$	$trpy^{0/-1}$	$trpy^{-1/-2}$	
ferrocene		0.41			437 (96), 322 (56)
tpy			<−1.7		278
Fctpy		0.57	<−1.7		459 (0.91), 364 (2.2), 280 (28), 248 (28)
pytpy					310 (8.3), 275 (27), 242 (43)
$Ru(tpy)_2^{2+}$	1.19		−1.19	−1.52	478 (14), 306 (61), 269 (39)
$Ru(tpy)(Fctpy)^{2+}$	1.42	0.59	−1.21	−1.52	515 (sh), 478 (15), 306 (61), 270 (41)
$Ru(Fctpy)_2^{2+}$	1.39	0.58	−1.22	−1.52	526 (15), 482 (15), 310 (60), 284 (44), 274 (49)
$Ru(pytpy)_2^{2+}$					488 (27), 309 (59), 275 (75), 240 (47)
$Fe(Fcty)_2^{2+}$	1.11	0.57			587 (23), 318 (51), 283 (47), 276 (45)
$Zn(Fctpy)_2^{2+}$		0.62			526 (5.8), 404 (3.6), 321 (44), 285 (48)

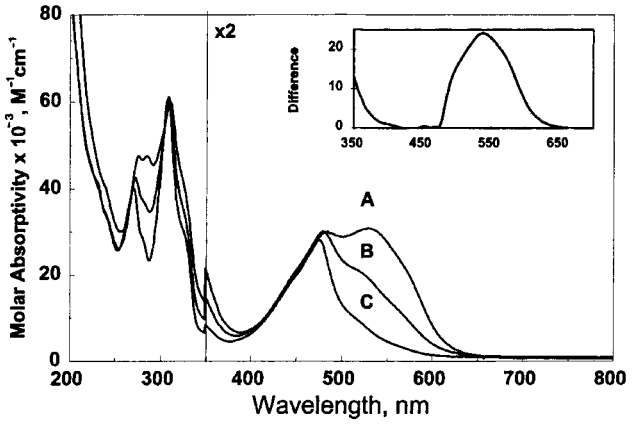

Figure 1. UV-visible absorption spectra of (A) $Ru(Fctpy)_2^{2+}$, (B) $Ru(tpy)(Fctpy)^{2+}$, (C) $Ru(tpy)_2^{2+}$ in acetonitrile solution at room temperature. Inset: difference spectrum (A)−(C).

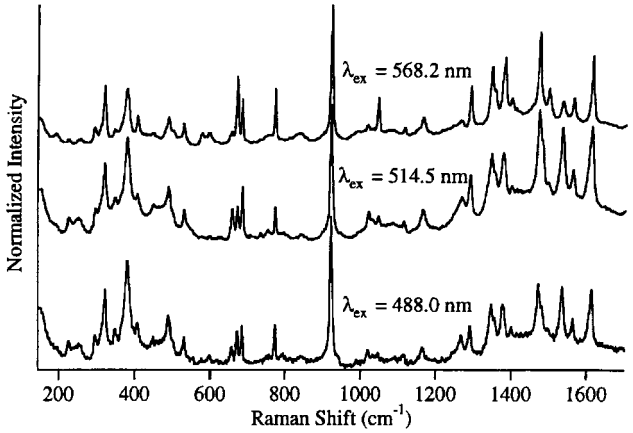

Figure 2. Resonance Raman spectra of $Ru(Fctpy)_2^{2+}$ in acetonitrile solution using various wavelengths for excitation.

the association of the terpyridyl nitrogens with a cationic center, such as Ru^{2+}, Zn^{2+}, Ni^{2+}, or H^+ lowers the energy of the π_{tpy}* orbitals giving rise to an intense transition in the visible region. The $Fe(Fctpy)_2^{2+}$ complex possesses an absorption band at 587 nm (ϵ = 23 000 M^{-1} cm^{-1}), which is red-shifted and more intense than that observed for $Fe(tpy)_2^{2+}$ (λ_{max} = 562 nm, ϵ = 12 000 $M^{-1}cm^{-1}$).[49,50] The observed absorption manifold for $Fe(Fctpy)_2^{2+}$ appears to be composed of $^1[(d(\pi)_{Fe})^6] \rightarrow {}^1[(d(\pi)_{Fe}{}^5\ (\pi^*_{tpy})^1]$ and $^1[(d(\pi)_{Fc})^6] \rightarrow {}^1[(d(\pi)_{Fc})^5(\pi^*_{tpy}{}^{Fe})^1]$ MLCT transitions.

Attempts were made to observe the outer-sphere $^1[(d(\pi)_{Fc})^6] \rightarrow {}^1[(d(\pi)_{Fc})^5\ (\pi^*_{tpy}{}^{Ru})^1]$ charge-transfer transition in an ion-paired $Ru^{II}(tpy)_2^{2+}$//Fc complex, eq 4. New transitions that may

$$Ru^{II}(tpy)_2^{2+}//Fc \rightarrow Ru^{II}(tpy)(tpy^{\bullet-})^{+}//Fc^{+} \qquad (4)$$

be assigned to the OSCT band were not evident in room-temperature acetonitrile solution with $[Ru^{II}(tpy)_2^{2+}] = 10^{-5}$ M and [Fc] < 10^{-1} M in a 1 cm cell.

There is further information for the $^1[(d(\pi)_{Ru})^6] \rightarrow {}^1[(d(\pi)_{Ru})^5\ (\pi^*_{tpy}{}^{Fc})^1]$ and $^1[(d(\pi)_{Fc})^6] \rightarrow {}^1[(d(\pi)_{Fc})^5\ (\pi^*_{tpy}{}^{Ru})^1]$ transitions from the resonance Raman spectra of $Ru(Fctpy)_2^{2+}$ collected at different excitation wavelengths. Resonance Raman spectra for $Ru(Fctpy)_2^{2+}$ obtained with 488.0, 514.5, and 568.2 nm excitation in acetonitrile solution (298 K) are shown in Figure 2. The Raman spectrum measured with 488.0 nm excitation for $Ru(Fctpy)_2^{2+}$ was identical to that obtained with 514.5 nm excitation and were found to be similar to the previously published resonance Raman spectra of $Ru(tpy)_2^{2+}$.[43,51] Previous studies on $Ru(bpy)_3^{2+}$ and $Os(bpy)_3^{2+}$ have shown that the bpy modes that experience the greatest enhancements are a series of symmetrical ν(bpy) vibrations from 1000 to 1600 cm^{-1}.[51] A similar enhancement pattern is apparent for $Ru(tpy)_2^{2+}$ as a series of low-energy Raman bands. Changing the excitation wavelength from 514.5 to 568.2 nm dramatically changes the intensity pattern of the Raman bands. The spectra were normalized to the Raman band of CH_3CN. The Raman band energies of $Ru(Fctpy)_2^{2+}$ along with data for $Ru(tpy)_2^{2+}$ are presented in Table S1 in the Supporting Information.

Photophysical Properties. The $Ru(tpy)_2^{2+}$*, $Ru(tpy)(Fctpy)^{2+}$*, and $Ru(Fctpy)_2^{2+}$* complexes were nonemissive in room-temperature fluid solution. Photophysical data measured in 4:1 (v/v) EtOH/MeOH glasses at 77 K demonstrated emission maxima ($\lambda_{max}{}^{em}$), emission quantum yields (Φ_{em}), and lifetimes (τ) for $Ru(tpy)(Fctpy)^{2+}$* and $Ru(Fctpy)_2^{2+}$* as well as $Ru(tpy)_2^{2+}$*. These data and comparative literature data for $Ru(tpy)(4\text{-}Etpy)_3^{2+}$* (Etpy = 4-ethylpyridine) and $Ru(bpy)_3^{2+}$* are given in Table 2. The emission quantum yield for $Ru(tpy)(Fctpy)^{2+}$* was small ($\Phi_{em} \approx 0.003$ at λ_{exc} = 460 nm) and emission assigned to the radiative decay of $Ru(Fctpy)_2^{2+}$* was undetectable (<0.003) (see below). These differ dramatically from results observed for $Ru(bpy)_3^{2+}$* and $Ru(tpy)_2^{2+}$* (Φ_{em} is 0.38 and 0.48, respectively). Excited-state decay for $Ru(tpy)(Fctpy)^{2+}$* and $Ru(Fctpy)_2^{2+}$* could not be resolved with our nanosecond laser flash emission apparatus (τ < 25 ns; k_{obsd} > 4×10^7 s^{-1}). A number of attempts were made to measure the 77 K excited-state lifetimes for $Ru(tpy)(Fctpy)^{2+}$* and $Ru(Fctpy)_2^{2+}$* employing picosecond phase-shift fluorometric techniques. These experiments were unsuccessful because the emission intensities from $Ru(tpy)(Fctpy)^{2+}$* and $Ru(Fctpy)_2^{2+}$* were too weak.

The emission spectral manifold of $Ru(tpy)(Fctpy)^{2+}$* was qualitatively similar to that of $Ru(tpy)_2^{2+}$* with a 1250−1300

(49) Braterman, P. S.; Song, J.-I.; Peacock, R. D. *Inorg. Chem.* **1992**, *31*, 555.
(50) Krumholz, P. *Inorg. Chem.* **1965**, *4*, 612.
(51) Hansen, P. W.; Jensen, P. W. *Spectrochim. Acta* **1994**, *50A*, 169.

Table 2. Emission and Lifetime Data in 4:1 EtOH/MeOH (v/v) at 77 K

complex	λ_{max}^{em}, nm[a]	Φ_{em}	τ, μs
$[Ru(bpy)_3](PF_6)_2$	584, 630	0.38[b]	5.2
$[Ru(tpy)_2](PF_6)_2$	599, 648	0.48[c]	11.0
$[Ru(tpy)(4\text{-}Etpy)_3](PF_6)_2$[d]	634, 689		7.5
$[Ru(tpy)(Fctpy)](PF_6)_2$	601, 646	~0.003	<0.025
$[Ru(Fctpy)_2](PF_6)_2$	599, 648	<0.003[e]	<0.025
$[Ru(Fcphtpy)_2](PF_6)_2$[f]	n.o.[g]	n.o.[g]	n.o.[g]

[a] λ_{max} for the first vibronic components. [b] Demas, J. N.; Crosby, G. A. *J. Am. Chem. Soc.* **1971**, *93*, 2841. [c] (a) Stone, M. L.; Crosby, G. A. *Chem. Phys. Letts.* **1981**, *79*, 5479. [d] Data from ref 43. [e] It cannot be ruled out at the present time that the weak emission arises from $[Ru(tpy)_2](PF_6)_2$. To give this result the level of the impurity would have to be <0.54%. [f] Data from ref 10. [g] n.o. = not observed.

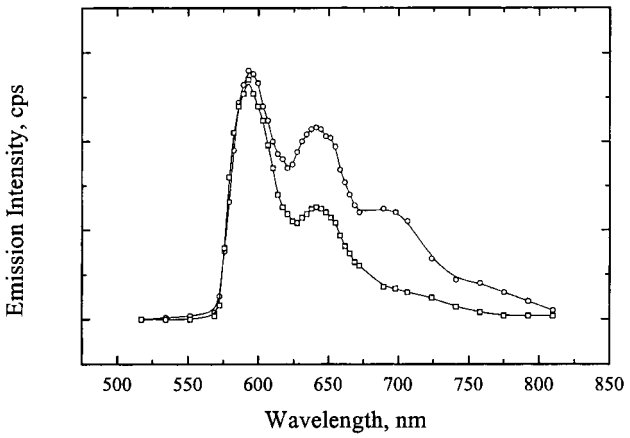

Figure 3. Emission spectra for (a) $Ru(tpy)_2^{2+}$* (□) and (b) $Ru(tpy)(Fctpy)^{2+}$* (○).

cm^{-1} vibronic progression. However, the emission maxima of the first vibronic progression at 601 nm for $Ru(tpy)(Fctpy)^{2+}$* was slightly red-shifted relative to $Ru(tpy)_2^{2+}$* as judged from normalized emission spectra collected under identical experimental conditions, Figure 3. More significantly, the ratio of intensities of the first and second vibronic components of the emission manifolds for $Ru(tpy)(Fctpy)^{2+}$* ($I_{646}/I_{601} = 0.77$) was larger than that observed for $Ru(tpy)_2^{2+}$* where $I_{648}/I_{599} = 0.47$. These features were independent of excitation and monitoring wavelengths employed. The differences in the emission spectra of $Ru(tpy)(Fctpy)^{2+}$* and $Ru(tpy)_2^{2+}$* and the significantly shorter excited-state lifetimes suggest that emission from $Ru(tpy)(Fctpy)^{2+}$* is intrinsic. Excitation spectral data for the $Ru(tpy)(Fctpy)^{2+}$* were independent of monitoring wavelength and resemble those observed for $Ru(tpy)_2^{2+}$* with no evidence for a $^1[(d(\pi)_{Fc})^6] \rightarrow {}^1[(d(\pi)_{Fc})^5\ (\pi^*_{tpy}{}^{Ru})^1]$ charge-transfer band which is observed in the room-temperature absorption spectrum. Excitation into the 530 nm $^1[(d(\pi)_{Fc})^6] \rightarrow {}^1[(d(\pi)_{Fc})^5\ (\pi^*_{tpy}Ru)^1]$ charge-transfer band for $Ru(Fctpy)_2^{2+}$* does not lead to population of an emissive state.

Normalized excitation and emission spectral profiles for $Ru(Fctpy)_2^{2+}$* overlay exactly with that observed for $Ru(tpy)_2^{2+}$*. The weak luminescence observed for samples of $Ru(Fctpy)_2^{2+}$* is likely due to trace amounts of $Ru(tpy)_2^{2+}$* which emit strongly at this temperature. Based on the observed quantum yields, the level of $[Ru(tpy)_2](PF_6)_2$ in solid samples of $[Ru(Fctpy)_2](PF_6)_2$ is <0.6%.

Experiments were carried out to assess the room-temperature photochemical stability of the Fctpy assemblies. Bulk photolysis of acetonitrile or dichloromethane solutions of Fctpy leads to very slow spectral changes, resulting in the growth of a band at 590 nm. With $Ru(Fctpy)_2^{2+}$ and $Ru(tpy)(Fctpy)^{2+}$, photolysis results in a loss of intensity in the band at 530 nm. These changes are consistent with the slow photochemical breakdown of the ferrocenyl moiety and, when possible, the released Fe^{2+} is coordinated to any available tpy site. Under the same thermal conditions, the Fctpy species are stable. Breakdown of the ferrocenyl unit, as evidenced by formation of $Fe(tpy)_2{}^{2+}$-type species, has been observed under various synthetic conditions. These types of reactions which lead to decomposition of the ferrocenyl unit have been observed previously.[23,40]

Discussion

The Krönhke synthetic methodology[52] has proven to be a convenient and versatile route to synthesizing substituted terpyridine species. In the present study, terpyridine species containing redox-active or auxiliary coordinating sites have been prepared and used in the synthesis of a variety of metal complexes. The compounds reported here represent an addition to a class of heterobimetallic bichromophoric Fe/Ru and CN bridged Ru/Rh complexes which possess an MLCT Ru(II) polypyridyl chromophore donor covalently coupled to an acceptor moiety with low-lying metal-centered excited states.[53−57] The results of the UV−visible and emission spectroscopic investigations as well as the resonance Raman experiments provide some detailed insight into the excited-state dynamics of $Ru(tpy)(Fctpy)^{2+}$ and $Ru(Fctpy)_2{}^{2+}$.

Franck−Condon MLCT States. The complexes $Ru(tpy)_2{}^{2+}$, $Ru(tpy)(Fctpy)^{2+}$, and $Ru(Fctpy)_2{}^{2+}$ exhibit intense $^1[(d(\pi)_{Ru})^6)] \rightarrow {}^1[(d(\pi)_{Ru})^5(\pi^*_{tpy})^1]$ bands in the 490 nm region of the visible absorption spectra. Well-defined low-energy shoulders on the $^1[(d(\pi)_{Ru})^6)] \rightarrow {}^1[(d(\pi)_{Ru})^5(\pi^*_{tpy})^1]$ MLCT band envelopes are observed between 500 and 650 nm ($\epsilon = \sim 100-400\ M^{-1}\ cm^{-1}$) for $Ru(tpy)_2{}^{2+}$ and $Ru(tpy)(4\text{-}Etpy)_3{}^{2+}$ analogues as well as $Ru(bpy)_3{}^{2+}$ where $\epsilon \approx 100\ M^{-1}\ cm^{-1}$. These bands have been previously assigned to $^1[(d(\pi)_{Ru})^6)] \rightarrow {}^3[(d(\pi)_{Ru})^5(\pi^*_{tpy})^1]$ transitions which become partially allowed due to spin−orbit coupling, which has the effect of mixing the singlet and triplet excited-state manifolds.[43,44] The molar absorptivities of the triplet-based $^1[(d(\pi)_{Ru})^6)] \rightarrow {}^3[(d(\pi)_{Ru})^5(\pi^*_{tpy})^1]$ transitions appear to be larger in the tpy-based chromophores because of enhanced mixing with low-lying $\pi\pi^*$ states on the tpy ligand.[43]

The $Ru(tpy)(Fctpy)_2{}^{2+}$ and $Ru(Fctpy)_2{}^{2+}$ complexes have intense, broad structureless $^1[(d(\pi)_{Fc})^6] \rightarrow {}^1[(d(\pi)_{Fc})^5\ (\pi^*_{tpy}{}^{Ru})^1]$ charge-transfer transitions which obscure the weaker $^1[(d(\pi)_{Ru})^6)] \rightarrow {}^3[(d(\pi)_{Ru})^5(\pi^*_{tpy})^1]$ Ru-based singlet−triplet transitions. Resonance Raman spectra[43,54] support the assignment of tpy orbitals as the acceptor site for the 530 nm $^1[(d(\pi)_{Fc})^6] \rightarrow {}^1[(d(\pi)_{Fc})^5\ (\pi^*_{tpy}{}^{Ru})^1]$ charge-transfer transition. The intensity observed for a resonance Raman band is derived from the underlying electronic transitions. Enhancements occur for Raman bands which undergo equilibrium displacement between ground and excited states for corresponding normal modes. By tuning the laser source to the wavelength of different electronic transitions, the nature of the transition can be discerned by the Raman bands which demonstrate enhanced intensities.[43,54]

(52) Kröhnke, F. *Synthesis* **1976**, 1.
(53) Thompson, D. W.; Wallace, A. W.; Swayambunathan, V.; Endicott, J. F.; Petersen, J. D.; Ronco, S. E.; Hsiao, J.-S.; Schoonover, J. R. *J. Phys. Chem. A.* **1997**, *101*, 8152.
(54) Scandola, F.; Argazzi, R.; Bignozzi, C. A.; Indelli, M. T. *J. Photochem. Photobiol. A: Chem.* **1994**, *82*, 191.
(55) Moore, K. J.; Lee, L.; Figard, J. E.; Gelroth, J. A.; Stinson, A. J.; Wohlers, H. D.; Petersen, J. D. *J. Am. Chem. Soc.* **1983**, *105*, 2274.
(56) Larson, S. L.; Hendrickson, S. M.; Ferrere, S.; Derr, D. L.; Elliot, C. M. *J. Am. Chem. Soc.* **1995**, *117*, 5881.
(57) Scheml, R. H.; Auerbach, R. A.; Wacholtz, W. F.; Elliott, C. M.; Freitag, R. A.; Merkert, J. W. *Inorg. Chem.* **1986**, *25*, 2440.

For $Ru(Fctpy)_2^{2+}$, resonance Raman spectra, measured with 488.0 and 514.5 nm excitation, possess the same pattern of bands. Over 30 bands are identified between 100 and 1700 cm^{-1} in these spectra. This number compares to 23 bands observed for $Ru(tpy)_2^{2+}$ in the same region with 457.9 nm excitation into the Ru−tpy MLCT transition (Figure 2 and Table S1 in Supporting Information). Many of the bands in the spectra of $Ru(Fctpy)_2^{2+}$ are analogous to bands for $Ru(tpy)_2^{2+}$. The slight differences in band energies and number of bands can be attributed to the 4′-substituted tpy compared to an unsubstituted tpy. The data are consistent with the assignment of the absorption feature near 480 nm in $Ru(Fctpy)_2^{2+}$ as an Ru−tpy MLCT transition as in $Ru(tpy)_2^{2+}$.

Excitation at 568.2 nm for $Ru(Fctpy)_2^{2+}$ results in a similar resonance Raman spectrum as with higher energy excitation (Figure 2) but with some major differences. This exciting line is far enough removed from the 480 nm transition that only the near resonance effects should be evident. However, the tpy bands still demonstrate significant intensity, but with a different pattern of enhancement. For example, Raman bands at 578, 596, 670, 771, 1045, and 1497 cm^{-1} undergo intensity enhancement of greater than a factor of 2 with 568.2 nm excitation compared with 488.0 or 514.5 nm excitation. A major loss in Raman intensity is also observed for bands at 656, 1265, 1479, and 1533 cm^{-1} in the 568.2 nm spectrum. These major differences suggest a different underlying transition, yet a transition involving π^*_{tpy} for the absorption feature at 526 nm. The Raman data are consistent with the assignment of a $^1[(d(\pi)_{Fc})^6] \rightarrow {}^1[(d(\pi)_{Fc})^5\ (\pi^*_{tpy}{}^{Ru})^1]$ transition.

A $^1[(d(\pi)_{Fc})^6] \rightarrow {}^1[(d(\pi)_{Fc})^5\ (\pi^*_{tpy}{}^{Ru})^1]$ transition may be present for $[Ru(Fcphtpy)_2](PF_6)_2$[24] (Fcphtpy = 4′-(4-ferrocenyl)-phenyl-2,2′;6′,2″-terpyridine) (λ_{max} = 501 nm; ϵ = 34 800 M^{-1} cm^{-1}). However, the intensity of this Fc-based charge-transfer transition appears significantly smaller. The phenylene spacer in $[Ru(Fcphtpy)_2](PF_6)_2$ effectively increases the distance between the Fc donor and Ru(tpy) acceptor sites. Therefore, the $^1[(d(\pi)_{Fc})^6] \rightarrow {}^1[(d(\pi)_{Fc})^5\ (\pi^*_{tpy}{}^{Ru})^1]$ charge-transfer transition intensity is decreased. The opposite trend has been observed in the following polyene-bridged Ru(II)/Fc.[48] In these systems, intense $^1[(d(\pi)_{Fc})^6] \rightarrow {}^1[(d(\pi)_{Fc})^5\ (\pi^*_{bpy}{}^{Ru})^1]$ charge-transfer transitions are observed at 523 nm (ϵ = 10 300 M^{-1} cm^{-1}) and 536 nm (ϵ = 33 500 M^{-1} cm^{-1}) for $[Ru(bpy)_2$(polyene-Fc (4))$]^{2+}$ and $[Ru(bpy)_2$(polyene-Fc (5))$]^{2+}$, respectively. The enhanced intensity seems to arise from unusually high electronic coupling over long distances provided by the rigid "conductive" polyene spacer group.

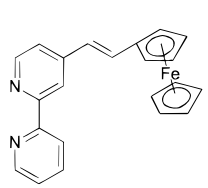

Polyene-Fc(4)

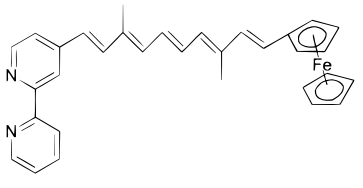

Polyene-Fc(5)

Electronic Coupling. The factors which influence the strength of electronic coupling between covalently bound donor−acceptor complexes have been the focus of intense study.[10,53−62] The strength of electronic coupling is reflected by the magnitude of the electronic matrix element, H_{RP}.[58] In the weak coupling limit where the magnitude of H_{RP} is small, the donor and acceptor moieties are essentially isolated and the resulting donor−acceptor complex displays properties which are essentially a sum of the individual components. In the other extreme, where H_{RP} is large, the donor−acceptor complex is electronically delocalized with properties very different from the component monomers. Even though the Ru−tpy chromophoric donor and ferrocenyl acceptor in the Ru(Fctpy) assemblies appear to be "strongly coupled" by means of the tpy−cp linkage, in many respects these systems behave as independent donor−acceptor systems. The energies of the $^1[(d(\pi)_{Ru})^6)] \rightarrow {}^1[(d(\pi)_{Ru})^5(\pi^*_{tpy})^1]$ transitions and $Ru^{III/II}$ reduction potentials in the $Ru(tpy)_2^{2+}$, $Ru(tpy)(Fctpy)^{2+}$, and $Ru(Fctpy)_2^{2+}$ complexes are quite similar to component mononuclear species based on the visible absorption and electrochemical data (Table 1). Even oxidation of the Fc substituents to Fc^+ sites to produce $Ru(Fctpy)_2^{4+}$ and $Ru(tpy)(Fctpy)^{3+}$ was shown to have minimal effect on the $Ru^{III/II}$ redox couple and the $^1[(d(\pi)_{Ru})^6)] \rightarrow {}^1[(d(\pi)_{Ru})^5(\pi^*_{tpy})^1]$ absorption band in the visible spectrum. Therefore, presumably the Ru−tpy energetics are also little effected by changes in the pendant Fc. The substantial additivity of the spectroscopic and electrochemical properties indicate a relatively weak degree of metal−metal electronic coupling in the ground state.

An interesting feature in the visible absorption spectrum of $Ru(Fctpy)_2^{2+}$ is that both the $^1[(d(\pi)_{Ru})^6] \rightarrow {}^1[(d(\pi)_{Ru})^5\ (\pi^*_{tpy}{}^{Fc})^1]$ and $^1[(d(\pi)_{Fc})^6] \rightarrow {}^1[(d(\pi)_{Fc})^5\ (\pi^*_{tpy}{}^{Ru})^1]$ transitions terminate on the intervening tpy ligand with comparable intensities, even though the degree of charge transfer is expected to differ between these two MLCT transitions. The absorption intensity is determined by the magnitude of the transition dipole moment μ_{12} along the charge centroid axis.[62] Experimentally, μ_{12} may be estimated from the oscillator strength, f, of the charge-transfer band as related by eqs 5 and 6.

$$f = (4.61 \times 10^{-9})\epsilon_{max}(\Delta\nu_{1/2}) \quad (5)$$

$$f = (1.08 \times 10^{-5})\nu_{max}\mu^2 \quad (6)$$

The quantities ϵ_{max}, $\Delta\nu_{1/2}$, and ν_{max} in eqs 5 and 6 are the extinction coefficient, the full width at half-maximum, and the energy of the CT band, respectively. From the Gaussian deconvolution[63] of the visible spectrum of $Ru(tpy)_2^{2+}$ (Figure 1C) and the difference of the $Ru(Fctpy)_2^{2+}$ and $Ru(tpy)_2^{2+}$ spectra (Figure 1, inset), oscillator strengths of 0.31 and 0.27 were estimated for the $^1[(d(\pi)_{Ru})^6] \rightarrow {}^1[(d(\pi)_{Ru})^5\ (\pi^*_{tpy}{}^{Fc})^1]$ and the $^1[(d(\pi)_{Fc})^6] \rightarrow {}^1[(d(\pi)_{Fc})^5\ (\pi^*_{tpy}{}^{Ru})^1]$ transitions, respectively. Using these quantities and values for ν_{max} of 20,700, and 19 000 cm^{-1} for the $^1[(d(\pi)_{Ru})^6] \rightarrow {}^1[(d(\pi)_{Ru})^5\ (\pi^*_{tpy}{}^{Fc})^1$ and $^1[(d(\pi)_{Fc})^6] \rightarrow {}^1[(d(\pi)_{Fc})^5\ (\pi^*_{tpy}{}^{Ru})^1]$ transitions, respectively, the transition dipole moments are 1.39 and 1.32 eÅ for the respective transitions. The value of 1.39 eÅ for the $^1[(d(\pi)_{Ru})^6] \rightarrow {}^1[(d(\pi)_{Ru})^5\ (\pi^*_{tpy}{}^{Fc})^1]$ transition in $Ru(Fctpy)_2^{4+}$ is slightly larger than the value of 1.13 eÅ calculated for the $^1[(d(\pi)_{Ru})^6] \rightarrow {}^1[(d(\pi)_{Ru})^5\ (\pi^*_{tpy})^1]$ transition in an analogous $Ru(ph\text{-}tpy)_2^{4+}$ system described elsewhere.[6] Creutz, Newton, and Sutin[62] have

(58) Lei, Y.; Buranda, T.; Endicott, J. F. *J. Am. Chem. Soc.* **1990**, *112*, 8820.
(59) Richardson, D. E.; Taube, H. *J. Am. Chem. Soc.* **1983**, *105*, 40.
(60) Oevering, H.; Verhoeven, J. W.; Paddon-Row: M. N.; Warman, J. M. *Tetrahedron* **1989**, *45*, 4751.
(61) Chen, P. Y.; Meyer, T. J. *Chem. Rev.* **1998**, *98*, 1439.
(62) Cruetz, C.; Newton, M. D.; Sutin, N. *J. Photochem. Photobiol. A: Chem.* **1994**, *82*, 47.
(63) The $^1[(d(\pi)_{Ru})^6)] \rightarrow {}^1[(d(\pi)_{Ru})^5(\pi^*_{tpy})^1]$ MLCT band was adequately fit with three Gaussian curves. The oscillator strength was calculated using the ϵ_{max} and $\Delta\nu_{1/2}$(abs) derived from the largest contributing Gaussian band which was found to contribute 85% of the total MLCT band envelope.

related the transition dipole moment to the electronic coupling element, H_{ab}, by the equation

$$\mu = eH_{ab}\mathbf{r}_{ab}/h\nu_{max} \quad (7)$$

where $\mathbf{r}_{ab}$ is the donor−acceptor charge-center separation and e is the unit electrical charge. The center-to-center distance for the $^1[(d(\pi)_{Ru})^6] \rightarrow {}^1[(d(\pi)_{Ru})^5\ (\pi^*_{tpy}{}^{Fc})^1]$ oscillator is 2.5 Å.[2] A center-to-center distance of 5 Å, the distance from Fc to the center of the tpy ligand found in the published structure of Fctpy,[11,12] was used for the $^1[(d(\pi)_{Fc})^6] \rightarrow {}^1[(d(\pi)_{Fc})^5\ (\pi^*_{tpy}{}^{Ru})^1]$ oscillator. Using these values, eq 7, and correcting for a statistical factor of 2, the values of H_{ab} are calculated to be 4.9×10^3 cm^{-1} and 2.2×10^3 cm^{-1} for the $^1[(d(\pi)_{Ru})^6] \rightarrow {}^1[(d(\pi)_{Ru})^5\ (\pi^*_{tpy}{}^{Fc})^1]$ and $^1[(d(\pi)_{Fc})^6] \rightarrow {}^1[(d(\pi)_{Fc})^5\ (\pi^*_{tpy}{}^{Ru})^1]$ oscillators, respectively.

The magnitude of H_{ab} is governed by the nature of the ground- and excited-state wave functions and how well these functions are mixed.[59−61] In the absence of molecular orbital calculations, these factors cannot be rigorously evaluated. Qualitatively, however, the larger electronic coupling element for the $^1[(d(\pi)_{Ru})^6] \rightarrow {}^1[(d(\pi)_{Ru})^5\ (\pi^*_{tpy}{}^{Fc})^1]$ transition is consistent with a higher degree of metal−ligand overlap between the Ru(II)-centered orbitals and tpy-centered orbitals than between the Fc-centered orbitals and the trpy-centered orbitals. The magnitude of H_{ab} in the $^1[(d(\pi)_{Fc})^6] \rightarrow {}^1[(d(\pi)_{Fc})^5\ (\pi^*_{tpy}{}^{Ru})^1]$ transition is expected to be maximized when the cp−tpy moieties in $Ru(Fctpy)_2{}^{2+}$ are coplanar. In the solid state, the interannular twist angle between the cyclopentadienyl ring and the central pyridine of Fctpy is 19.2°.[11,12] Rotation about the cp−tpy axis is expected to be facile in room-temperature fluid solution and most of the rotomers of the pendant Fc will not be coplanar with the tpy moiety, resulting in a lower orbital overlap between Fc and tpy.

Excited-State Decay. Attachment of the Fc moiety to the tpy has minimal influence on the ground-state spectroscopic and electrochemical properties of the heterobimetallic donor−acceptor when compared to the monomeric components. However, the rates of nonradiative decay are significantly enhanced in $Ru(tpy)(Fctpy)^{2+}$* and $Ru(Fctpy)_2{}^{2+}$* relative to $Ru(tpy)_2{}^{2+}$*.

Because electronic coupling between the Ru(II) and Fc centers is small (see above), the $Ru(tpy)_2{}^{2+}$ ion is a good model for the Ru(II) terpyridyl chromophore in $Ru(tpy)(Fctpy)^{2+}$* and $Ru(Fctpy)_2{}^{2+}$*. From the data of Crosby,[33] the MLCT excited-state of $Ru(tpy)_2{}^{2+}$ consists of a manifold of three low-lying states, all having appreciable triplet character, and all significantly populated at 77 K and room temperature.[10,33] The excited-state lifetime of $Ru(tpy)_2{}^{2+}$* at 77 K is 11 μs, substantially longer than that found $Ru(bpy)_3{}^{2+}$*. The longer lifetime is attributed to delocalization of the excited electron over the larger tpy framework.[43] Above 90 K, the lifetime of $Ru(tpy)_2{}^{2+}$* is strongly temperature dependent because low-lying metal-centered states provide additional pathways for excited-state decay.[10,43,45] The very short lifetimes observed for $Ru(tpy)(Fctpy)^{2+}$* and $Ru(Fctpy)_2{}^{2+}$* at 77 K are attributed to the presence of Fc which provides additional channels for excited-state decay. A comprehensive excited-state energy level diagram is presented in Figure 4, showing the typical Ru−tpy states on the left and the expected states arising from the presence of the Fc moiety on the right. The numerical values are estimates using experimental data obtained under different conditions, and some caution is warranted in their interpretation. Using spectroscopic information, the energetics of the $^1[(d(\pi)_{Ru})^6)] \rightarrow {}^1[(d(\pi)_{Ru})^5(\pi^*_{tpy}{}^{Fc})^1]$ and $^1[(d(\pi)_{Fc})^6] \rightarrow {}^1[(d(\pi)_{Fc})^5\ (\pi^*_{tpy}{}^{Ru})^1]$ Franck−Condon excited-states, designated $^1[Ru^{III}(tpy^{-\bullet})Fc^{II}]$ and $^1[Ru^{II}$-

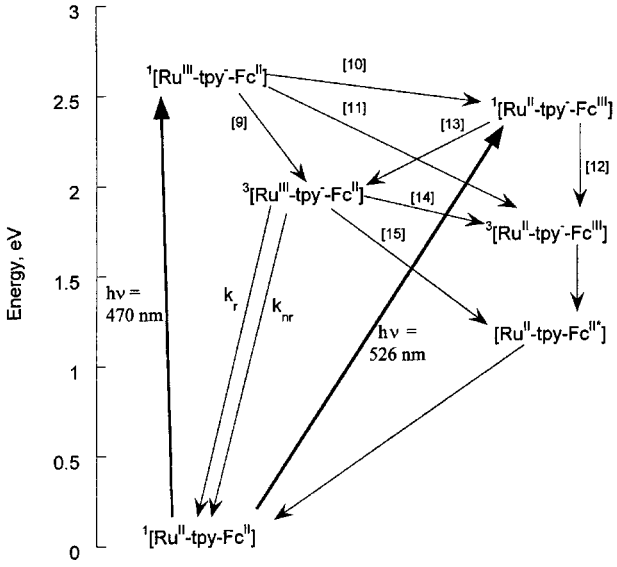

Figure 4. Energy level diagram for $Ru(tpy)_x(Fctpy)_{2-x}{}^{2+}$ complexes.

$(tpy^{-\bullet})Fc^{III}]$ in Figure 4, are estimated to be 2.6 and 2.3 eV, respectively. The energy of the emitting $^3[Ru^{III}(tpy^{-\bullet})Fc^{II}]$ state was taken to be 2.1 eV estimated by drawing a tangent to the high-energy side of the first vibronic progression in the emission spectra of $Ru(tpy)(Fctpy)^{2+}$* shown in Figure 3. An energy of 1.9 eV for the $^3[Ru^{II}(tpy^{-\bullet})Fc^{III}]$-based state was estimated from the low-energy onset of the $^1[(d(\pi)_{Fc})^6] \rightarrow {}^1[(d(\pi)_{Fc})^5\ (\pi^*_{tpy}{}^{Ru})^1]$ absorption band.[48] The lowest lying state is expected to be ferrocene triplet excited state, $^3[Ru^{II}(tpy)Fc^{II*}]$, at an energy somewhere between 1.1 and 1.8 eV.[10]

The rate constant for excited-state decay mediated by Fc in $Ru(tpy)(Fctpy)_2{}^{2+}$ can be estimated assuming that k_r and k_{nr}, the rate constants for radiative and nonradiative relaxation from the Ru-based ^{3}[MLCT] state of $Ru(tpy)(Fctpy)^{2+}$, are similar to those for $Ru(tpy)_2{}^{2+}$. Then the differences in excited-state lifetimes between $Ru(tpy)(Fctpy)^{2+}$* and $Ru(tpy)_2{}^{2+}$* are due to Fc-mediated quenching. Under these conditions, k_q is given by

$$k_q = (\tau)^{-1} - (\tau_o)^{-1} \quad (8)$$

where τ is the lifetime of $Ru(tpy)(Fctpy)^{2+}$* ($\tau < 25$ ns) and τ_o is the lifetime of $[Ru(tpy)_2]^{2+}$* ($\tau_o = 11$ μs). Therefore, $k_q \geq 4 \times 10^7$ s^{-1}.

Examination of the energy level diagram shown in Figure 4 reveals a number of exogonic processes that may be accessed following excitation into the $^1[(d(\pi)_{Ru})^6)] \rightarrow {}^1[(d(\pi)_{Ru})^5(\pi^*_{tpy}{}^{Fc})^1]$ based and lower energy $^1[(d(\pi)_{Fc})^6] \rightarrow {}^1[(d(\pi)_{Fc})^5\ (\pi^*_{tpy}{}^{Ru})^1]$ MLCT bands. Excitation into the 470 nm $[(d(\pi)_{Ru})^6)] \rightarrow {}^1[(d(\pi)_{Ru})^5(\pi^*_{tpy}{}^{Fc})^1]$ band leads to the formation of the $^1[Ru^{III}$-$(tpy^{-\bullet})Fc^{II}]$ Franck−Condon state, and a number of pathways are available for excited-state decay, eqs 9−11.

$$^1[Ru^{III}(tpy^{-\bullet})Fc^{II}] \rightarrow {}^3[Ru^{III}(tpy^{-\bullet})Fc^{II}], \quad \Delta E = -0.5 \text{ eV} \quad (9)$$

$$^1[Ru^{III}(tpy^{-\bullet})Fc^{II}] \rightarrow {}^1[Ru^{II}(tpy^{-\bullet})Fc^{III}], \quad \Delta E = -0.3 \text{ eV} \quad (10)$$

$$^1[Ru^{III}(tpy^{-\bullet})Fc^{II}] \rightarrow {}^3[Ru^{II}(tpy^{-\bullet})Fc^{III}], \quad \Delta E = -0.7 \text{ eV} \quad (11)$$

Low-energy excitation into the 530 nm $^1[(d(\pi)_{Fc})^6] \rightarrow {}^1[(d(\pi)_{Fc})^5\ (\pi^*_{tpy}{}^{Ru})^1]$ band leads to the formation of the $^1[Ru^{II}(tpy^{-\bullet})Fc^{III}]$

Franck−Condon state, which then may relax via eqs 12 and 13.

$$^1[Ru^{II}(tpy^{-\bullet})Fc^{III}] \rightarrow {}^3[Ru^{II}(tpy^{-\bullet})Fc^{III}], \quad \Delta E = -0.4 \text{ eV} \tag{12}$$

$$^1[Ru^{II}(tpy^{-\bullet})Fc^{III}] \rightarrow {}^3[Ru^{III}(tpy^{-\bullet})Fc^{II}], \quad \Delta E = -0.2 \text{ eV} \tag{13}$$

The presence of a low-lying Fc-centered metal triplet state, designated $^3[Ru^{II}(tpy)Fc^{II}*]$ in Figure 4, has been implicated in other bimolecular and intramolecular quenching studies involving Ru(II) polypyridyl chromophores and Fc.[10,64,65] A similar state should be present in the Ru(tpy)(Fctpy)$^{2+}$ and Ru(Fctpy)$_2{}^{2+}$ assemblies studied here. However, these states are spectroscopically invisible, and therefore their exact energies are unknown.

The precise mechanism of excited-state decay cannot be deduced from the emission spectra alone. However, the following information can be extracted from the existing data. Following 470 nm excitation, $^1[Ru^{III}(tpy^{-\bullet})Fc^{II}]$ decays rapidly to $^3[Ru^{III}(tpy^{-\bullet})Fc^{II}]$ (eq 9), $^3[Ru^{II}(tpy^{-\bullet})Fc^{III}]$ (eq 11), or to $^1[Ru^{II}(tpy^{-\bullet})Fc^{III}]$ (eq 10). The latter, if formed, must decay rapidly to form $^3[Ru^{II}(tpy^{-\bullet})Fc^{III}]$ (eq 12), $^3[Ru^{III}(tpy^{-\bullet})Fc^{II}]$ (eq 13), or $^3[Ru^{II}(tpy)Fc^{II}*]$. If the $^3[Ru^{III}(tpy^{-\bullet})Fc^{II}]$ state forms by any of the above processes, rapid nonradiative relaxation via Fc-based excited states occurs (eq 14 or 15).

$$^3[Ru^{III}(tpy^{-\bullet})Fc^{II}] \rightarrow {}^3[Ru^{II}(tpy^{-\bullet})Fc^{III}], \quad \Delta E = -0.2 \text{ eV} \tag{14}$$

$$^3[Ru^{III}(tpy^{-\bullet})Fc^{II}] \rightarrow {}^3[Ru^{II}(tpy)Fc^{II}*], \quad \Delta E = -0.3 \text{ to } -1.0 \text{ eV} \tag{15}$$

The excitation spectrum of Ru(tpy)(Fctpy)$^{2+}$* (λ_{mon} at 620 and 660 nm) closely resembles the absorption spectrum of Ru(tpy)$_2{}^{2+}$ with no evidence of the $^1[(d(\pi)_{Fc})^6] \rightarrow {}^1[(d(\pi)_{Fc})^5 (\pi^*_{tpy}{}^{Ru})^1]$ transition at 526 nm in 4:1 EtOH/MeOH at 77 K. This and the effective quenching of the emission for Ru(tpy)(Fctpy)$^{2+}$ and Ru(Fctpy)$_2{}^{2+}$ compared to Ru(tpy)$_2{}^{2+}$ suggests that the $^3[Ru^{III}(tpy^{-\bullet})Fc^{II}]$ state may well form (eq 9), but it decays rapidly via eq 14 or 15. The absence of an $^1[(d(\pi)_{Fc})^6] \rightarrow {}^1[(d(\pi)_{Fc})^5 (\pi^*_{tpy}{}^{Ru})^1]$ CT transition in the excitation profile requires that excitation into the 530 nm band results in very fast relaxation of the $^1[Ru^{II}(tpy^{-\bullet})Fc^{III}]$ state to form an electronically excited nonemissive species such as $^3[Ru^{II}(tpy^{-\bullet})Fc^{III}]$* or $^3[Ru^{II}(tpy)Fc^{II}*]$. Other systems, such as $[(CN)_4Fe(dpp)Ru(bpy)_2]$ (dpp = 2,3-bis(2-pyridyl)pyrazine), have shown very different excited-state behavior depending excitation wavelengths.[53] There is also precedence for ultrafast ^{1}[MLCT] − ^{5}[LF] (DS = 2) nonradiative relaxation (τ < 800 fs) in the Fe(II) spin crossover systems.[66] Furthermore, the wavelength-dependent resonance Raman studies on [Ru(Fctpy)$_2$]$^{2+}$* show that the vibronic structures for the $[Ru^{III}(tpy^{-\bullet})Fc^{II}]$ and $[Ru^{II}(tpy^{-\bullet})Fc^{III}]$ CT excited states differ dramatically. For the $[Ru^{II}(tpy^{-\bullet})Fc^{III}]$ excited state there is a significant increase in the number of vibrations which are resonantly enhanced during the $^1[(d(\pi)_{Fc})^6] \rightarrow {}^1[(d(\pi)_{Fc})^5 (\pi^*_{tpy}{}^{Ru})^1]$ CT excitation. By inference, the Franck−Condon vibrational overlap factors which couple the ground and excited states may be enhanced and provide a facile route to nonradiative decay from the $[Ru^{II}(tpy^{-\bullet})Fc^{III}]$ CT excited state to repopulate the $^1[Ru^{II}(tpy)Fc^{II}]$ ground state.

Acknowledgments are made to the Natural Science and Engineering Research Council of Canada (NSERC) for a postdoctoral fellowship to D.W.T. for portions of this work completed at the Department of Chemistry, University of North Carolina at Chapel Hill, Chapel Hill, NC and to Prof. Thomas J. Meyer for helpful discussions and generously providing access to his spectroscopy laboratory. Resonance Raman experiments were performed at Los Alamos National Laboratory under the auspices of the U.S. Department of Energy with funding from The University of California Directed Research and Development Program to J.R.S.

Supporting Information Available: Table S1 lists the Raman Band Energies for Ru(tpy)$_2{}^{2+}$ and Ru(Fctpy)$_2{}^{2+}$. This material is available free of charge via the Internet at http://pubs.acs.org.

IC980798B

(64) Hammarström, L.; Barrigelleti, F.; Flamingni, L.; Indelli, M. T.; Armaroli, N.; Calogero, G.; Guardigli, M.; Sour, A.; Collin, J.-P.; Sauvage, J.-P *J. Phys. Chem. A* **1997**, *101*, 9061.

(65) Wrighton, M. S.; Pdungsap. L.; Morse, D. L. *J. Phys. Chem.* **1975**, *79*, 66. Lee, E. J.; Wrighton, M. S. *J. Am. Chem Soc.* **1991**, *113*, 8562.

(66) McCusker, J. K.; Walda, K. N.; Dunn, R. C.; Simon, J. D.; Magde, D.; Hendrickson, D. N. *J. Am. Chem. Soc.* **1993**, *115*, 298.